Fate and transport of petroleum hydrocarbons in engineered biopiles in polar regions

M.J. Whelan[1], F. Coulon[2*], G. Hince[3], J. Rayner[4], R. McWatters[3], T. Spedding[3], I. Snape[3]

[1]Department of Geography, University of Leicester, Leicester, LE1 7RH, UK

[2] Department of Environmental Science and Technology, School of Applied Sciences, Cranfield University, College Road, Cranfield, Bedfordshire, MK43 0AL, UK

[3] Risk and Remediation, Terrestrial and Nearshore Ecosystems, Australian Antarctic Division, Kingston, Tasmania, Australia, 7050

[4]CSIRO, Land and Water, Private Bag No. 5, Wembley, Western Australia 6913, Australia

[*]Corresponding author. Dr Frederic Coulon

Email: f.coulon@cranfield.ac.uk

Abstract

A dynamic multi-media model that includes temperature-dependency for partitioning and degradation was developed to predict the behaviour of petroleum hydrocarbons during biopiling at low temperature. The activation energy (*Ea*) for degradation was derived by fitting the Arrhenius equation to hydrocarbon concentrations from temperature-controlled soil mesocosms contaminated with crude oil and diesel. The model was then applied to field-scale biopiles containing soil contaminated with diesel and kerosene at Casey Station, Antarctica. Temporal changes of total petroleum hydrocarbons (TPH) concentrations were very well described and predictions for individual hydrocarbon fractions were generally acceptable (disparity between measured and predicted concentrations was less than a factor two for most fractions). Biodegradation was predicted to be the dominant loss mechanism for all but the lightest aliphatic fractions, for which volatilisation was most important. Summertime losses were significant, resulting in TPH concentrations which were about 25% of initial concentrations just one year after the start of treatment. This contrasts with the slow rates often reported for hydrocarbons *in situ* and suggests that relatively simple remediation techniques can be effective even in Antarctica.

Key Words: Fugacity model; Hydrocarbon contamination; Antarctic soils; Biopile

1. Introduction

Petroleum hydrocarbon contamination has been identified as a significant environmental problem in the polar and sub-polar regions, particularly in areas with permanent settlements or bases (Gore et al., 1999; Snape et al., 2006; Tin et al., 2009). Hydrocarbon pollutants in cold soils can remain for long periods because biodegradation is often limited by temperature (Bradley and Chapelle, 1995; Boethling et al., 2009). Hydrocarbons can also ultimately migrate into adjacent marine systems where they can pose risks to sensitive ecosystems (Poland et al., 2003; Snape et al., 2006). It is important, therefore, to investigate the potential effectiveness of different remediation techniques which can be challenged by the harsh environmental conditions and by the substantial logistical difficulties of working in remote locations (Mumford et al., 2013).

Of the various treatment methods available for the remediation of hydrocarbon-contaminated soil, “biopiling” is being increasingly considered. In this technique, contaminated soil is excavated and piled up above ground, sometimes with added nutrients and sometimes with enhanced aeration. Leaching losses of hydrocarbons with appreciable aqueous solubility and low vapour pressure are usually controlled by placing the pile on an impermeable surface and then capturing and treating any leachate produced (Coulon et al., 2012). Biopiles are technically straightforward and relatively cheap to construct and have been shown to be effective in temperate zone studies (Coulon et al., 2010a). Even in cold regions the activity of microbial degraders has been recognised as being seasonally significant (Coulon et al., 2005; Sanscartier et al., 2009) and may, therefore, have potential for hydrocarbon remediation provided factors such as aeration, temperature and nutrient supply are not limiting. That said,

68 practical implementation of biopiling at field scale remains relatively untested in cold
69 regions.
70 In any environmental technology it is useful to understand the interactions between
71 environmental and process variables in order to optimise operational management.
72 Multimedia fate and transport models allow such interactions to be explored and can
73 be used to predict the environmental concentrations and associated deleterious effects
74 of pollutants (Whelan, 2013).
75 In this paper, the behaviour of petroleum hydrocarbons in polar and sub-polar
76 biopiled soils was investigated using the dynamic fugacity-based model developed by
77 Coulon et al. (2010b) which was modified to allow for the temperature-dependence of
78 partition coefficients and degradation rate constants. Despite widespread
79 acknowledgement of the influence of temperature on hydrocarbon biodegradation
80 (Atlas and Bartha, 1992; Margesin and Schinner, 1999; Gibb et al., 2001; Ferguson et
81 al., 2003a; Coulon et al., 2005) and environmental phase partitioning (Mackay and
82 Arnot, 2011) temperature-dependence is sometimes ignored. Although previous work
83 has been conducted to model the behaviour of hydrocarbon fractions in cold
84 environments, this has largely been empirical, rather than mechanistic.
85
86 **2. Methods**
87 The temperature dependency of degradation was parameterised using experimental
88 data obtained from laboratory-scale biopiles of sub-Antarctic soils contaminated with
89 diesel fuel and crude oil near the Port aux Français station on Kerguelen Island
90 (Coulon et al., 2005). The parameterised model was then applied to field-scale
91 biopiles at Casey Station, Antarctica, in order to evaluate model performance and to

help with the interpretation of observed data on hydrocarbon behaviour in these systems.

2.1 Model description

Briefly, the model considers an evaluative four-phase environmental system containing: (1) mineral solids; (2) organic matter, including any non-aqueous phase liquid (NAPL); (3) air and (4) water. Dimensions of the system are set to represent the biopile under consideration (Coulon et al., 2010b). The behaviour of each hydrocarbon fraction (*i*) is considered separately via the following mass balance equation, expressed in terms of fugacity (Mackay, 2001):

$$\frac{dM_i}{dt} = E_i - D_{Ti} \cdot f_i \qquad (1)$$

where M is the mass of the fraction remaining (mol), E (mol h^{-1}) is the emission rate (i.e. the rate of hydrocarbon fraction added to the biopile, which in our case is zero), D_T is the total "D" value (mol Pa^{-1} h^{-1}), t is time (h) and f is the fugacity (Pa) of the fraction in the biopile at a given time. The predicted total petroleum hydrocarbon (TPH) concentration is assumed to be the sum of the modelled concentrations of individual fractions. It is assumed that all phases within the biopile have equal fugacity (i.e. they are always in thermodynamic equilibrium: Paterson et al., 1994; Di Guardo et al., 1994). D-values represent loss rates due to advection out of the system and reaction within the system. The product of D and f gives a mass transfer in mol h^{-1}. D_T is calculated as the sum of the D-values for individual process rates:

$$D_T = D_A + D_V + D_L + D_R \quad (2)$$

where D_A represents loss in air by advection laterally through the system (e.g. by blowing air through the soil); D_V represents combined chemical diffusion through the air- and water- filled pore space, followed by loss via volatilisation; D_L represents leaching loss and D_R represents loss by reaction (biodegradation).

Equation (1) differs slightly from the dynamic equation used by Coulon et al. (2010b), which was expressed in terms of the fugacity change per unit time i.e.:

$$\frac{df_i}{dt} = -\frac{D_{T\,i}.f_i}{V_T.Z_{BULK\,i}} \quad (3)$$

where V_T is the total volume of the system considered. This is because fugacity capacity values (Z_{BULK}) change with temperature so fugacity increases are possible when partition coefficients change, resulting in mass balance errors when we explicitly account for the effect of temperature. Further details of the concepts and other equations used can be found in Coulon et al. (2010b). The model was coded in Microsoft Visual Basic for Applications (VBA).

2.2. Temperature dependence of partition coefficients and degradation rate

The temperature dependence of chemical partitioning between phases in the model was represented by:

$$K_{XY}(T_e) = K_{XY}(T_r).\exp\left(\frac{\Delta U_{XY}}{R}.\left(\frac{1}{T_r} - \frac{1}{T_e}\right)\right) \quad (4)$$

where $K_{XY}(T_e)$ is the partition coefficient between phase *X* and phase *Y*, at the temperature (T_e, K) of the environmental compartments under consideration; $K_{XY}(T_r)$ is the partition coefficient, at the reference temperature (T_r), which is usually 298 K; ΔU_{XY} is the energy of phase transfer or solvation enthalpy (J mol^{-1}) and *R* is the gas constant (J mol^{-1} K^{-1}). An attempt was made to estimate values of ΔU_{XY} from relevant literature. In the case of ΔU_{OW} (which was assumed to be equal to ΔU_{OC}) very little has been reported and a value of -20 kJ mol^{-1} was assumed based on Foster et al. (2005). This explicitly assumes that hydrophobicity (K_{OW} and K_{OC}) decreases with increasing temperatures. A range of values for ΔU_{AW} were based on the temperature-dependence of vapour pressure derived from Foster et al. (2005) which, in turn, employed Trouton's rule (Hand, 1994) to derive the enthalpy of vaporisation from the boiling point (Table 1). Although aqueous solubility also changes with temperature, this variation tends to be compound-specific, confounding the development of a general rule for temperature correction (Foster et al., 2005). The errors introduced by the failure to adjust aqueous solubility and vapour pressure simultaneously are not systematic and are considered tolerable.

Temperature adjustments were made to degradation rate constants using the Arrhenius equation:

$$k(T_e) = k(T_r).\exp\left(\frac{Ea}{R}.\left(\frac{1}{T_r} - \frac{1}{T_e}\right)\right) \quad (5)$$

where $k(T_e)$ is the rate constant at the environmental temperature, T_e (K); $k(T_r)$ is the rate constant at the reference temperature, T_r (usually 298 K) and Ea is the activation energy (J mol^{-1}). The value of $k(T_r)$ is calculated from the half-life at the reference temperature (HL_r), assuming first order kinetics:

$$k(T_r) = \frac{\ln(2)}{HL_r} \quad (6)$$

Reference half-life values in soil were estimated by Coulon et al. (2010b) using algorithms in the Estimation Program Interface (EPI) Suite™ (Syracuse Research Corp., http://www.syrres.com/esc/est_soft.htm) for a range of different member compounds within equivalent carbon numbers fractions.

There is empirical evidence that a limited amount of biodegradation can continue in frozen soils if there is an unfrozen water fraction (which will depend, in part, on the pore size distribution associated moisture release curve). However, once the temperature falls below about -5 °C (Rike et al., 2003), degradation is often limited by the diffusion of nutrients and waste products, even if some microbes are still metabolically active (Rivkina et al., 2000; Harvey et al., 2012). Degradation was, therefore, assumed to be zero below -4°C. Similarly, chemical diffusion in water and air was assumed to be limited by physical barriers in the soil at temperatures below -2 °C (Gibb et al., 2001) which can limit volatile losses if moisture content is high. Although Biggar et al. (1998) suggest that NAPL can migrate into permafrost via gravity drainage and capillary suction into ice-free soil pores, most hydrocarbon fractions considered here are already partitioned within the soil matrix and, therefore, are unlikely to move in the same way.

186

187 **2.3 Estimation of activation energy from laboratory-scale biopile data**

188 Values for *Ea* were derived for various hydrocarbon fractions from laboratory-scale
189 experimental data measured in sub-Antarctic soils from Kerguelen Island (49º 21'S,
190 70 º 13'E). Data on the fractions are given in the Supplementary Information (Tables
191 S1 and S2). Briefly, duplicate soil biopiles contaminated with either diesel or Blend
192 Arabian Light crude oil (BAL) were incubated at 4, 10 and 20°C. Each biopile
193 contained 5 kg of sandy loam soil with a moisture content of 40% (w/w), a pH of 6.4,
194 an organic carbon content of 15.8% and a bulk density of 1134 kg m^{-3}. Biopiles were
195 homogenised manually twice a month. Hydrocarbon fractions in soil were quantified
196 by gas chromatography coupled to a mass spectrometer (GCMS), as described by
197 Coulon et al. (2005), at the onset of the experiment and after 42, 90 and 180 days.
198 Concentration changes were normalised against natural biomarkers (hopane and
199 chrysene) which are involatile and which are recalcitrant to biodegradation. Although
200 the biopiles were not covered, losses are assumed to be due to biodegradation rather
201 than to volatilisation because (i) the fractions examined had relatively low volatility;
202 (ii) losses of most fractions increased when fertiliser was added (suggesting a nutrient
203 limitation to biodegradation) and (iii) the abundance of hydrocarbon-degrading
204 microorganisms increased markedly in contaminated soil compared with
205 uncontaminated controls (Coulon et al., 2005). Nevertheless some volatilisation will
206 have occurred and it is conceivable that this resulted in an over-estimation of
207 biodegradation rate constants for some fractions. These data are assumed to be
208 appropriate for deriving the temperature-dependency of the model described here
209 because they were derived from soils with microbial communities which have
210 evolved for cold environments and which may, therefore, have similarities to cold soil

communities elsewhere. Values of *Ea* were derived for each fraction via a two-step process, assuming that each fraction in the mixture was assumed to behaves independently: (i) first order kinetic equations were fitted to observed changes in the concentration of the fraction concerned over time at each temperature (4, 10 and 20 °C) by least squares optimisation to yield a rate constant at each temperature; (ii) a value of *Ea* was derived for each fraction by plotting the rate constants against incubation temperature and performing another least-squares optimisation of Equation (6).

2.4 Field scale biopile of Antarctic fuel-contaminated soil

Casey Station (66°17' S, 110°31' E) is situated on an ice-free peninsula in Antarctica (Mumford et al., 2013). In 1999, a fuel spill (*ca.* 2000 litres) resulted in soil contamination with 80% Arctic Blend diesel (Bergen distillate) and 20% Aviation Turbine Kerosene (ATK) (Snape et al., 2006). Contaminated soil from this spill was excavated and placed in five biopiles during the 2010-11 summer season. The dimensions and physical properties of each biopile system are provided in Table 2. Biopile 5 was smaller and was set up to evaluate the effects of passive aeration compared with using a vacuum air-extraction system (Biopiles 1 to 4) which periodically draws air from the soil to a network of perforated PVC pipes and a granular activated carbon (GAC) trap. All biopiles were established on geosynthetic liners and were covered in a permeable geotextile to mitigate off-site dust migration whilst allowing for air inflow and evaporation of water. A leachate recirculation system was used to recycle any leachate. Snow was removed at the beginning of the summer season to prevent introduction of melt water into the biopiles. With little moisture delivered to the biopiles in the form of precipitation (the average water-

equivalent precipitation is 210 mm; Mumford et al., 2013), the introduction of water is considered small. The rate of water transfer was therefore set to an arbitrary value of 10 mm yr^{-1} (i.e. 10 L $m^{-2}y^{-1}$).

Contaminated soil was placed in the biopiles in 0.5 m lifts and sampled at each lift in a grid pattern (0.5, 1.0 and 1.5 m). Between 35 and 46 soil samples per biopile were collected and stored at -20^{o}C prior to analysis by gas chromatography as described by Snape et al., (2006). The initial TPH concentration ranged between 2655 and 4216 mg kg^{-1} for all five biopiles. This refers to the total area under the chromatogram and includes resolvable peaks plus an unresolved complex mixture representing a range compounds at various stages of degradation. Sampling was repeated in November and December 2011 and February 2012 using an excavator to cut into the biopiles (25-36 samples per biopile). After each sampling the biopiles were turned by excavator. The concentrations of each fraction for each biopile are shown in Table 2.

The average temperature recorded in Biopile 1 was used to adjust partition coefficients and degradation rate constants (Figure 1). Note that temperature data were unavailable for the first 48 days of the experiment. Temperatures for this period were therefore sampled randomly from a normal distribution with a mean of -5.32 ºC and a coefficient of variation of 0.2. In November and December 2012 the average soil temperature was -3 ºC at 1 m from the base and -7 ºC at 0.5 m from the base suggesting that these assumptions are reasonable. It was assumed that biodegradation was not affected by nutrient availability, since they were added to each biopile, although it is possible that nutrients may have been locally limiting.

2.5 Sensitivity Analysis

A classical one-at-a-time sensitivity analysis (Whelan, 2013) was carried out, in which parameters were varied systematically one at a time over a range, with other factors held at their base (best estimate) values. Two sets of parameters were investigated: (i) chemical properties (K_{AW}, K_{OC}, Ea, $k(T_r)$, ΔU_{OW} and ΔU_{AW} where $_{AW}$ refers to air and water, $_{OC}$ refers to organic carbon and water, $_{OW}$ refers to octanol and water) and (ii) environmental properties (G_A, G_L, k_v, z, f_{OC}, ρ_B, f_{air}, f_{wat} where G_A and G_L are flow rates for air and water, k_v is the partial mass transfer coefficient on the air side of the air-soil interface, z is the pile depth, f_{OC} is the organic carbon content of the soil, ρ_B is the bulk density and f_{air} and f_{wat} are the volume fractions of air and water, respectively, which are used in the calculation of the diffusion coefficients in pore water and pore air). Other terms have been previously defined. The value of each parameter was increased and decreased in increments of 20% of its base value (with other parameters being set at their base values) and changes observed to the predicted time series of TPH concentration.

3. Results and Discussion

3.1 Energy of activation for the aliphatic and aromatic fractions

Changes in the concentration of hydrocarbon fractions at different temperatures together with the first-order best-fit curves are shown in the Supplementary Information (Figure S1). The 'best fit' values for the first order rate constant, k, are shown in Table 1.

First order kinetics appear to describe the time series data reasonably well (high r^2 values) for the aliphatic fractions investigated at all three temperatures considered. In contrast, the r^2 values of the EC_{12-16} and EC_{16-21} aromatic fractions at 10 and 20°C were lower than for the other fractions suggesting that degradation of these fractions

285 may not follow first order kinetics. For many compounds this could be due to
286 degradation by co-metabolism (Horvath, 1972; Horowitz and Atlas, 1977). As the
287 concentration of the easily degradable compounds decrease, the degradation rates of
288 other more recalcitrant compounds may also decrease (more than would be expected
289 from simply a decrease in overall microbial activity) such that removal of the residual
290 hydrocarbons becomes relatively slow. This type of interaction may be reflected in a
291 deviation of the degradation kinetics from first order (Tabak and Govind, 1997). This
292 is also supported by microcosm observations of ^{14}C-octadecane mineralisation in
293 Casey Station soils, reported by Ferguson et al. (2003a; b) in which the rate was
294 proportional to concentration raised to the power 1.5.
295 It is interesting to compare the minimum half-lives (i.e. derived from the maximum
296 value of the fitted rate constants – typically at 20 °C) for individual fractions derived
297 from the Kerguelen soil with the reference half-lives assumed for these fractions by
298 Coulon et al. (2010b), which were calculated from predicted half-lives in water
299 generated using EPI Suite™ (see above and Foster et al., 2005). The ratio of the
300 experimental half-life derived here (corrected to 25 °C by rearranging Equation 5) to
301 the estimated half-life given by Coulon et al. (2010b) is also shown in Table 1. With
302 the exception of the aliphatic EC_{12-16} fraction, the predicted half-life was within a
303 factor two of the experimental Kerguelen soil value, suggesting that the degradation
304 half-lives given by EPI Suite™ are probably a reasonable approximation.
305 Plots of the derived first order rate constants versus the reciprocal of temperature are
306 shown in the Supplementary Information (Figure S2). For both the EC_{10-12} aliphatic
307 and EC_{10-12} aromatic fractions, there is a strong relationship between rate constant and
308 temperature, which is well described by the Arrhenius equation. However, for the
309 other fractions especially the aliphatic EC_{16-35} and the aromatic EC_{16-21} and EC_{21-35}

fractions, the rate constants appear to be higher at 10 °C than at 20 °C suggesting that the optimum temperature for degradation is lower than 20 °C and that the Arrhenius equation may not always be applicable. This is not altogether unexpected in soils in which the microbial community will have adapted to low temperatures (see also Colwell et al., (1978) who observed higher hydrocarbon degradation rates at 3 ºC than at 22 ºC). In any case, where temperature-dependence for the degradation of a fraction is weak (i.e. where *Ea* is low) or where the relative concentration of the fraction is low, the ability of Equation 5 to reproduce the temperature-dependence of the observed rate constant may not be that important.

The 'best fit' *Ea* values for the aromatic EC_{21-35} fraction (diesel and BAL) and the aromatic EC_{12-16} for BAL were negative (i.e. the rate constants decrease with increasing temperature). In the model, *Ea* values for these fractions were set to zero (Table 1). In the case of the aromatic EC_{21-35} fraction, *Ea* was negative for both diesel and crude oil treatments and was, therefore, set to zero in the model. This will have the effect of maintaining a high rate constant for the predicted biodegradation of this fraction (i.e. the reference half-life will be unaffected by temperature above -4 °C: see Section 2.2). For the other fractions, the average *Ea* values for diesel and BAL were employed. In general, for equivalent carbon numbers, the *Ea* values for the aromatic fractions were higher than for the aliphatic fractions (Table 1).

3.2 Predicting hydrocarbon persistence in Casey Station biopiles

Predicted TPH concentrations remaining in the Casey biopiles over time are shown in Figure 1, together with the mean measured values. Although the predicted concentrations of the different fractions in each biopile are different, the proportions of TPH remaining are similar, since the D-values used in the model to describe the

losses of each fraction were assumed to be the same. The average daily temperature data used to moderate the partition coefficients and degradation rate constants are also shown. Predicted concentration changes over the winter period when temperatures were well below freezing (as low as -20º C) were assumed to be negligible. However, as soon as temperatures increased to over -4 °C in spring, predicted hydrocarbon biodegradation and volatilisation re-commenced and the TPH concentration decrease was significant. Also shown in Figure 1 is the predicted TPH remaining with no temperature adjustment whatsoever and the predicted TPH remaining assuming no temperature adjustment in degradation and partition coefficients (i.e. with Ea, ΔU_{OC} and ΔU_{AW} set to zero) but assuming that degradation and volatilisation are switched off at low temperatures.

Overall, the pattern of predicted decrease in TPH matched the measured data reasonably well. This is encouraging, given the simple nature of the model and the assumptions made, although it should be noted that hydrocarbon concentrations in contaminated soil can be highly variable which means that the sampling error on the measured data could be considerable. Taking into account the temperature dependency of the partition coefficients and degradation rate constants was essential. Even though the patterns of hydrocarbon loss could be broadly represented simply by switching off volatilisation and degradation at low temperatures, full temperature-adjustment markedly improved the match with measured data.

Predicted changes in the concentrations of six different hydrocarbon fractions (aliphatic EC_{8-10} , EC_{10-12}, EC_{12-16} and $EC_{16-35;}$ aromatic EC_{10-12} and EC_{12-16}) in each of the five biopiles are shown in Figure 2. The model performance for individual fractions was also relatively good (within a factor two of the measured concentrations), although specific details suggest that the model description of loss

processes for some fractions is incomplete. For example, the model performance was reasonable for the aliphatic EC_{8-10} fraction (Figure 2a), over the first 7500 hours for Biopiles 4 and 5 but was poorer for the other biopiles, although the discrepancy was not consistent (almost no change in concentration was observed in Biopile 3 over the first 7500 hours, whereas for the other biopiles the model appeared to underestimate initial losses). Similarly, for the heavier aliphatic fraction (Figure 2c) predicted losses up to the first sampling appear to be reasonable, whereas the predicted overall summertime loss rate appears to be too high. This could be due to incorrect parameterisation or inappropriate model formulation (e.g. the simplifying assumption of first order kinetics or employing the Arrhenius equation with a reference temperature at 25 °C when microbial communities are adapted to different temperature optima). For the light aromatic fraction (Figure 2b), the model appeared to consistently underestimate the observed loss rate for all biopiles. Since biodegradation is the dominant loss process for this fraction (Table 3), this suggests that values for the reference degradation half-life and or for *Ea* may be too high.

One interesting feature apparent in Figure 2 is that observed concentrations of all fractions in Biopile 3 do not decrease between the start of the monitoring period and the first sampling but, thereafter, concentrations decrease at least as quickly as in the other systems. This is most apparent for the heavy aromatic fraction (Figure 2d) for which observed concentrations were higher at the first sampling compared with at the start. Whilst similar behaviour was observed for some fractions in other biopiles this was not consistent across fractions. There is currently no clear explanation for this behaviour, although it may simply reflect the heterogeneity of soil properties and hydrocarbon contamination within the biopiles which is not captured by the limited sample volume and number of soil samples collected. It should be noted that the soil

385 was still frozen when it was sampled in November 2011 but much of it had thawed by
386 December 2011. Furthermore, turning of the soil after each sampling may have
387 enhanced mixing and soil structure (i.e. enhanced porosity) which would contribute to
388 enhanced volatilisation and aerobic biodegradation. This also exposes different
389 volumes of soil to higher near-surface temperatures.
390 The relative performance of the model was quantified using the root mean squared
391 error (RMSE) between the measured and predicted concentrations for each fraction
392 (Table S3) and the average relative error (i.e. residual expressed as a percentage of
393 measured data: Table S4). In all biopiles, absolute errors are generally highest for the
394 aliphatic EC_{16-35} fraction (RMSE 11-43 mg kg^{-1}) and lowest for the aliphatic EC_{8-10}
395 fraction (RMSE 1.6-3.8 mg kg^{-1}) although average relative errors (which range
396 between 6% and 196%) are highest for the lighter fractions. In general, average
397 relative errors are less than 50% for most fractions.
398 Table 3 shows the predicted contribution of individual loss processes for the different
399 fractions in each biopile. For any individual fraction, the dominant loss process is
400 consistent across all five biopiles. For all fractions the predicted dominant loss
401 process is biodegradation except for the aliphatic EC_{8-10} fraction where volatilisation
402 was predicted to dominate. Volatilisation is alsopredicted to be important for the
403 aliphatic EC_{10-12} fraction (*ca*. 40% of total loss). The contributions of different
404 processes will reflect the relative magnitudes of the D-values, which in turn reflect
405 parameter values selected initially, such as degradation half-lives for the different
406 fractions in soil (Coulon et al., 2010b) and partial mass transfer coefficients for inter-
407 media transport. Since errors in assigning these parameter values will propagate into
408 predicted loss rates, Table 3 should be interpreted with caution. In particular, it
409 should be noted that an over-estimation of the biodegradation rate constant (e.g. as a

result of neglecting volatile losses in the mesocosm experiments) will result in an under-estimation of the relative contribution of volatilisation to overall loss. Table 3 also shows the measured and modelled average percentage lost after one year for different fractions. Model predictions are good for the aliphatic EC_{10-12} and EC_{12-16} and aromatic EC_{12-16} fractions but poor for the aliphatic EC_{16-35} and aromatic EC_{10-12} fractions. In the case of the aliphatic EC_{16-35} fraction the model over-estimates the loss but for the aromatic EC_{10-12} fraction the model significantly under-estimates the loss. The predicted dominance of biodegradation as a loss mechanism and the pattern of concentration changes observed over the course of the study suggest that microbial communities in the studied systems were able to begin to operate effectively at temperatures as low as -4 °C, which confirms observations by Gibb et al. (2001) and Rivkina et al. (2000) that soil microbes can be active as long as there are zones of liquid water in some of the pore space. The results also emphasise the importance of including the effects of temperature on organic chemical behaviour in environmental systems. Although losses appear to have been negligible for most fractions over the winter, summertime losses were significant. The TPH concentration after one year of treatment was approximately 25% of that at the start. Using the model to forecast TPH biodegradation (assuming the same temporal temperature pattern and no additional limitations in nutrient supply, water content or, for co-metabolised fractions, in the availability of degradable substrates) suggests that the mean TPH concentration at the end of year 2 will be of the order of <3% and that concentrations of all but the most recalcitrant individual fractions should be less than 4% (*ca* 20% in the case of the aromatic EC_{10-12} fraction).

3.3 Model Sensitivity

Figure 3 shows the influence of chemical–specific (Figure 3a) and system-specific (Figure 3b) parameters on the predicted TPH remaining in Biopile 1 after one year. Tabulated values and the average change in predicted TPH concentration per unit relative change in each parameter value are given in Table S5 of the SI. Of the chemical-specific parameters, the model is most sensitive to $k(T_r)$ and Ea, which control degradation, confirming the importance of biodegradation as a loss process. As Ea increases the percentage of TPH remaining increases, reflecting slower biodegradation due to greater temperature dependence. The TPH loss is also quite sensitive to the partition coefficients, H (the Henry's law coefficient) and K_{OC}. As H increases, the TPH remaining decreases, reflecting an increase in volatilisation, although volatile losses are also limited by the magnitude of mass transfer coefficients at the soil – atmosphere interface and by the fraction of water-filled pore space. As K_{OC} increases, the TPH remaining increases due to an increase in the predicted sorbed phase, which is assumed to be unavailable for volatile losses (but still available for biodegradation). Of the chemical parameters investigated, the model is least sensitive to the energies of phase change, ΔU_{OW} and ΔU_{AW}, although both parameters still exert an appreciable influence.

Of the system-specific parameters, f_{OC}, depth and f_{air} exert the most significant influence on the TPH remaining. An increase in f_{OC}, increases the sorbed phase concentration and reduces volatile losses, thereby increasing the TPH remaining. In the case of depth and f_{air}, their effect is due to their role in controlling volatilisation. An increase in pile depth is assumed to increase the diffusion path length – which decreases volatile losses vertically, although it also increases the cross sectional area through which air and associated vapours can travel laterally. An increase in f_{air} increases the available pore space through which vapour-phase hydrocarbons can

travel, increasing volatilisation and decreasing TPH remaining. Similarly, the model is moderately sensitive to the air flux rate G_A, which tends to enhance lateral vapour-phase transfers and reduce the TPH remaining. The model is insensitive to the water flux rate, G_L, reflecting the low fraction of TPH which is dissolved in the aqueous phase, or to the partial mass transfer coefficient on the air side of the air-soil interface, k_v, reflecting the fact that volatilisation is limited by factors inside the soil. Finally, the proportion of TPH remaining is insensitive to the soil bulk density (ρ_B), although ρ_B does affect the absolute magnitude of concentrations.

4 Conclusions

Our results demonstrate that biopiling can be a practical and effective remediation technique even under extreme Antarctic conditions. As expected, there was relatively little change in mean TPH concentration during the winter but during the summer, loss rates were high (average measured losses for individual fractions between 53 and 91% after one year: Table 3). These changes could be represented very well using a simple dynamic fugacity model provided that the temperature-dependence of partitioning and degradation was accounted for. This suggests that the values for *Ea* estimated from laboratory mesocosms may be broadly applicable to other polar and sub-polar soils. The ability of the model to accurately predict concentration changes for individual hydrocarbon fractions was much more variable especially for the aliphatic EC_{16-35} and aromatic EC_{10-12} fractions where model performance was unsatisfactory although the contribution of these fractions to TPH was relatively minor. A number of factors could explain poor model fits including the adoption of first order kinetics to describe non-first-order degradation, as well as sampling errors in the measured data. Additional experimental work is required to further investigate

484 the mechanisms for concentration changes in these fractions which may inform
485 improvements in the model. There is also still a need to test the model with more
486 empirical evidence of hydrocarbon fate and behaviour (e.g. of degradation metabolites
487 and via observations of changes in the ratio of different hydrocarbon isomers in
488 remediated systems) under a range of different climatic and edaphic conditions,
489 particularly at lower hydrocarbon concentrations. Future work should also seek to
490 normalise measured concentrations to conservative markers such as hopane (Coulon
491 et al., 2005; Prince et al., 2013) which can reduce the noise associated with variations
492 in absolute concentrations. One limitation of the work presented here is that model
493 validation was not possible for the two higher aromatic fractions (EC_{16-21} and EC_{21-35})
494 since these were not measured (reflecting low concentrations of these components in
495 the source oils). In future studies, the model should be tested on contaminated soils
496 containing these heavier aromatic components.
497
498 Overall, the model provides a useful tool that could help to guide remediation
499 decisions in cold environments contaminated with hydrocarbons. Losses were
500 predicted to be principally due to biodegradation (accounting for 76% of losses on
501 average for the fractions shown in Table 3 with volatilisation accounting for the
502 remainder). This challenges expectations of slow biodegradation in polar
503 environments and suggests that biopiling can be successfully used to treat
504 contaminated soils even at low temperatures. This is consistent with recent oil
505 biodegradation studies that simulate Arctic conditions (McFarlin et al. 2014).
506

Acknowledgements

This work was funded by the Australian Antarctic Division and was facilitated by a workshop held in Zermatt, Switzerland in 2012.

References

Atlas, R.M., Bartha, R., 1992. Hydrocarbon biodegradation and oil spill bioremediation. Adv. Microb. Ecol. 12, 287-338.

Biggar, K.W., Nahir, M., Haidar, S., 1998. Migration of petroleum contaminants into permafrost. Proceedings of the 7th International Permafrost Conference, Yellowknife, Canada

Boethling, R., Fenner, K., Howard, P., Klečka, G., Madsen, T., Snape, J.R., Whelan, M.J., 2009. Environmental persistence of organic pollutants: Guidance for development and review of POP risk profiles. Integr. Environ. Assess. Manage. 5, 539-556.

Bradley, P.M., Chapelle, F.H., 1995. Rapid toluene mineralization by aquifer microorganisms at Adak, Alaska: Implications for intrinsic bioremediation in cold environments. Environ. Sci. Technol. 29, 2778-2781.

Colwell, R.R.K., Mills, A.L., Walker, J. D., Garcia-Tello, P., Campos-P., V., 1978. Microbial ecology studies of the Metula spill in the Straits of Magellan. J. Fish. Res. Board Can. 35:573-580.

Coulon, F., Pelletier, E., Gourhant, L., Delille, D., 2005. Effects of nutrient and temperature on degradation of petroleum hydrocarbons in contaminated sub-Antarctic soil. Chemosphere. 58, 1439-1448.

531 Coulon, F., Al Awadi, M., Cowie, W., Mardlin, D., Pollard, S., Cunningham, C.,
532 Risdon, G., Arthur, P., Semple, K.T., Paton G.I., 2010a. When is a soil
533 remediated? Comparison of biopiled and windrowed soils contaminated with
534 bunker-fuel in a full-scale trial. Environ. Pollut. 158, 3032-3040.
535 Coulon, F., Whelan, M.J., Paton, G.I., Semple, K.T., Villa, R., Pollard, S.J.T., 2010b.
536 Multimedia fate of total petroleum hydrocarbon fractions in the soil:oil matrix of
537 constructed biopiles. Chemosphere. 81: 1454-1462.
538 Coulon, F., Brassington, K.J., Bazin, R., Linnet, P.E., Thomas, K.A., Mitchell, T.R.,
539 Lethbridge, G., Smith, J.W.N., Pollard, S.J.T., 2012. Effect of fertiliser
540 formulation and bioaugmentation on biodegradation and leaching of crude oils
541 and refined products in soils. Environ. Technol. 33, 1879-1893.
542 Ferguson, S.H., Franzmann, P.D., Snape, I., Revill, A.T., Trefry, M.G., Zappia, L.R.,
543 2003a. Effects of temperature on mineralisation of petroleum in contaminated
544 Antarctic terrestrial sediments. Chemosphere. 52, 975-987.
545 Ferguson, S.H., Franzmann, P.D., Revill, A.T., Snape, I., Rayner, J.L., 2003b. The
546 effects of nitrogen and water on mineralisation of hydrocarbons in diesel-
547 contaminated terrestrial Antarctic soils. Cold Reg. Sci. Technol. 37, 197-212.
548 Foster, K.L., Mackay, D., Parkerton, T.F., Webster, E., Milford, L., 2005. Five-stage
549 environmental exposure assessment strategy for mixtures: gasoline as a case
550 study. Environ. Sci. Technol. 39, 2711-2718.
551 Gibb, A., Chu, A., Kwong Wong, R.C., Goodman, R.H., 2001. Bioremediation kinetic
552 of crude oil at 5°C. J. Environ. Eng. 127, 818-823.
553 Gore, D.B., Revill, A.T., Guille, D., 1999. Petroleum hydrocarbons ten years after
554 spillage at a helipad in Bunger Hills, East Antarctica. Antarct. Sci. 11, 427-429.
555 Hand C.W., 1994. General Chemistry. Harcourt Brace & Company: Orlando, FL.

556 Harvey, A.N, Snape, I., Siciliano, S.D., 2012. Changes in liquid water alter nutrient
557 bioavailability and gas diffusion in frozen Antarctic soils contaminated with
558 petroleum hydrocarbons. Environ. Tox. Chem. 31, 395–401.
559 Horowitz, A., Atlas, R. M., 1977. Continuous open flow-through system as a model
560 for oil degradation in the Arctic Ocean. Appl. Environ. Microbiol. 33, 647-653.
561 Horvath, R.S., 1972. Microbial co-metabolism and degradation of organic compounds
562 in nature. Bacteriological Reviews 36, 146-155.
563 Mackay, D., 2001. Multimedia environmental models: the fugacity approach, second
564 edition. Lewis Publishers, MI.
565 Mackay, D., Arnott, J.A., 2011. The application of fugacity and activity to simulating
566 the environmental fate of organic contaminants. J. Chem. Eng. Data. 56, 1348-
567 1355.
568 Margesin, R., Schinner, F., 1999. Biological decontamination of oil spills in cold
569 environments. J. Chem. Technol. Biotechnol. 74, 381-389.
570 McFarlin, K.M., Prince, R.C., Perkins, R., Leigh, M.B., 2014. Biodegradation of
571 Dispersed Oil in Arctic Seawater at -1°C. PLoS ONE 9, e84297.
572 Mumford, K.A., Rayner, J.L., Snape, I., Stark, S.C., Stevens, G.W., Gore, D.B., 2013.
573 Design, installation and preliminary testing of a permeable reactive barrier for
574 diesel fuel remediation at Casey Station, Antarctica. Cold Reg. Sci. Technol. 96,
575 96-107.
576 Nair, D.R., Schnoor, J.L., 1994. Effect of soil conditions on model parameters and
577 atrazine mineralization rates. Water Res. 28, 1199-1205.
578 Poland, J.S., Riddle, M.J., Zeeb, B.A., 2003. Contaminants in the Arctic and the
579 Antarctic: a comparison of sources, impacts, and remediation options. Polar
580 Record 39, 369–383.

581 Prince, R.C., McFarlin, K.M., Butler, J.D., Febbo, E.J., Wang, F.C.Y., Nedwed, T.J.,
582 2013. The primary biodegradation of dispersed crude oil in the sea.
583 Chemosphere 90. 521–526.
584 Rike, A.G., Haugen, K.B., BØrresen, M., Engene, B., Kolstad, P., 2003. In situ
585 biodegradation of petroleum hydrocarbons in frozen arctic soils. Cold Reg. Sci.
586 Technol. 37, 97-120.
587 Rivkina, E.M., Friedmann, E. I., McKay, C.P., Gilichinsky, A.A., 2000. Metabolic
588 activity of permafrost bacteria below the freezing point. Appl. Environ. Microb.
589 66, 3230–3233.
590 Sanscartier, D., Zeeb, B., Koch, I., Reimer, K., 2009. Bioremediation of diesel-
591 contaminated soil by heated and humidified biopile system in cold climates.
592 Cold Reg. Sci. Technol. 55, 167-173.
593 Snape, I., Ferguson, S.H., Harvey, P. McA., Riddle, M.J., 2006. Investigation of
594 evaporation and biodegradation of fuel spills in Antarctica: II – Extent of natural
595 attenuation at Casey Station. Chemosphere. 63, 89-98.
596 Tabak, H.H., Govind, R., 1997. Protocol for determining bioavailability and
597 biokinetics of organic pollutants in dispersed, compacted and intact soil systems
598 to enhance *in situ* bioremediation. J. Ind. Microbiol. Biotechnol. 18, 330–339.
599 Tin, T., Fleming, Z.L., Hughes, K.A., Ainley, D.G. Convey, P., Moreno, C.A.,
600 Pfeiffer, S., Scott, J., Snape, I. 2009. Impacts of local human activities on the
601 Antarctic environment. Antarct. Sci. 21, 3-33.
602 Whelan, M.J., 2013. Predicting the fate and behaviour of cyclic volatile methyl
603 siloxanes in two contrasting North American lakes. Chemosphere. 91, 1566-
604 1576.
605

606

607 **Table 1:** Best-fit values of the degradation rate constant (*k*) and the energy of
608 activation (*Ea*) for the aliphatic and aromatic hydrocarbon fractions in hydrocarbon-
609 contaminated Kerguelen soil incubated at different temperatures. The half-life ratio is
610 the ratio of the minimum experimental half-life (corrected to 25 °C) to the half-life
611 derived from EPI Suite (Coulon et al., 2010b). Also shown is the value of ΔU_{AW}
612 assumed (based on the temperature-dependence of vapour pressure: Foster et al.,
613 2005).

614

615

Hydrocarbon fractions			***k*** **(d^{-1})**			**Half-life Ratio**	**Derived *Ea* ($kJ\ mol^{-1}$)**	**Assumed ΔU_{AW} ($kJ\ mol^{-1}$)**
			4°C	**10°C**	**20°C**			
Diesel fuel	**Aliphatic**	EC_{10-12}	0.036	0.037	0.040	0.968	4.72	8.48
		EC_{12-16}	0.011	0.017	0.015	2.260	5.80	9.06
		EC_{16-35}	0.009	0.014	0.013	1.650	8.40	10.70
	Aromatic	EC_{10-12}	0.009	0.016	0.026	0.494	36.68	8.48
		EC_{12-16}	0.007	0.024	0.018	0.730	12.50	9.06
		EC_{16-21}	0.006	0.008	0.008	1.460	8.86	10.62
		EC_{21-35}	0.006	0.006	0.004	0.963	0 (-19.9)	16.06
BAL crude oil	**Aliphatic**	EC_{10-12}	0.026	0.025	0.036	0.986	17.37	8.48
		EC_{12-16}	0.011	0.014	0.014	2.720	6.95	9.06
		EC_{16-35}	0.008	0.012	0.011	1.940	6.92	10.70
	Aromatic	EC_{10-12}	0.010	0.010	0.017	0.733	27.42	8.48
		EC_{12-16}	0.007	0.013	0.009	1.470	0 (-1.40)	9.06
		EC_{16-21}	0.002	0.004	0.006	1.600	37.72	10.62
		EC_{21-35}	0.005	0.008	0.004	0.722	0 (-19.64)	16.06

616

Table 2: Dimensions, soil properties and initial hydrocarbon concentrations in each biopile established on Casey Island. All biopiles had nutrients added, soil was turned over 3 times per year by excavator bucket and leachate was recirculated. Aeration was enhanced by vacuum pumps in Biopiles 1-4 but not in Biopile 5.

	Actively Remediated Biopiles				**Control**
	Biopile 1	**Biopile 2**	**Biopile 3**	**Biopile 4**	**Biopile 5**
Dimension and properties					
Total volume (m^3)	110	97	98	99	58
V_S (m^3)	73	65	65	66	39
V_W (m^3)	15	14	14	14	8
V_{NAPL} (m^3)	0.68	0.67	0.53	0.02	0.25
V_A (m^3)	21	18	18	19	11
Average % orgC	1	1	1	1	1
Soil density (kg m^{-3})	2400	2400	2400	2400	2400
Bulk density (kg m^{-3})	1600	1600	1600	1600	1600
Particle size fraction distribution (% dry matter basis)					
p > 9500 µm			44		
4750 > p < 9500 µm			9		
2000 > p < 4750 µm			9		
500 > p < 2000 µm			13		
63 > p <500 µm			14		
p < 63µm			12		
Nutrients					
N mg kg^{-1} soil	347	394	390	387	360
N:P ratio (soluble)	7.3	6	7.6	8.2	7.8
K:P ratio	1	1.1	1.1	1.1	1.1
N:P:K	7.3:1:1	6:1:1.1	7.6:1:1.1	8.2:1:1.1	7.8:1:1.1
Aliphatic concentrations (mg kg^{-1})					
EC_{8-10}	18	22	12	14	9
EC_{10-12}	156	193	124	126	102
EC_{12-16}	202	246	157	151	139
EC_{16-35}	173	208	157	153	133
Aromatic concentrations (mg kg^{-1})					
EC_{10-12}	11	13	8	8	7
EC_{12-16}	30	36	12	12	10
EC_{16-21}	0	0	0	0	0
EC_{21-35}	0	0	0	0	0
Ali+Aro (mg kg^{-1})	**590**	**717**	**470**	**464**	**400**
TPH (mg kg^{-1})	**3778**	**4216**	**3286**	**3231**	**2655**

Ali+Aro : Aliphatic + aromatic fractions; TPH: Total petroleum hydrocarbons

Table 3: The relative contribution of different loss processes to overall losses for different hydrocarbon fractions in different biopiles. Values in bold show the dominant loss process for each fraction. Also shown is the average measured and modelled % loss for each fraction.

		Aliphatic fractions				Aromatic fractions	
		EC_{8-10}	**EC_{10-12}**	**EC_{12-16}**	**EC_{16-35}**	**EC_{10-12}**	**EC_{12-16}**
Biopile 1	Volatilisation	**76**	38	10	1	12	1
	Leaching	0	0	0	0	0	0
	Degradation	24	**62**	**90**	**99**	**88**	**99**
Biopile 2	Volatilisation	**77**	39	10	1	13	1
	Leaching	0	0	0	0	0	0
	Degradation	23	**61**	**90**	**99**	**87**	**99**
Biopile 3	Volatilisation	**78**	40	11	1	13	1
	Leaching	0	0	0	0	0	0
	Degradation	22	**60**	**89**	**99**	**87**	**99**
Biopile 4	Volatilisation	**78**	40	11	1	13	1
	Leaching	0	0	0	0	0	0
	Degradation	22	**60**	**89**	**99**	**87**	**99**
Biopile 5	Volatilisation	**82**	47	14	1	18	1
	Leaching	0	0	0	0	0	0
	Degradation	18	**53**	**86**	**99**	**82**	**99**
Average Measured % Loss after 1 year		86.4	89.7	77.9	53.0	90.5	79.0
Average Modelled % Loss after 1 year		99.6	85.6	78.7	73.7	46.2	80.1

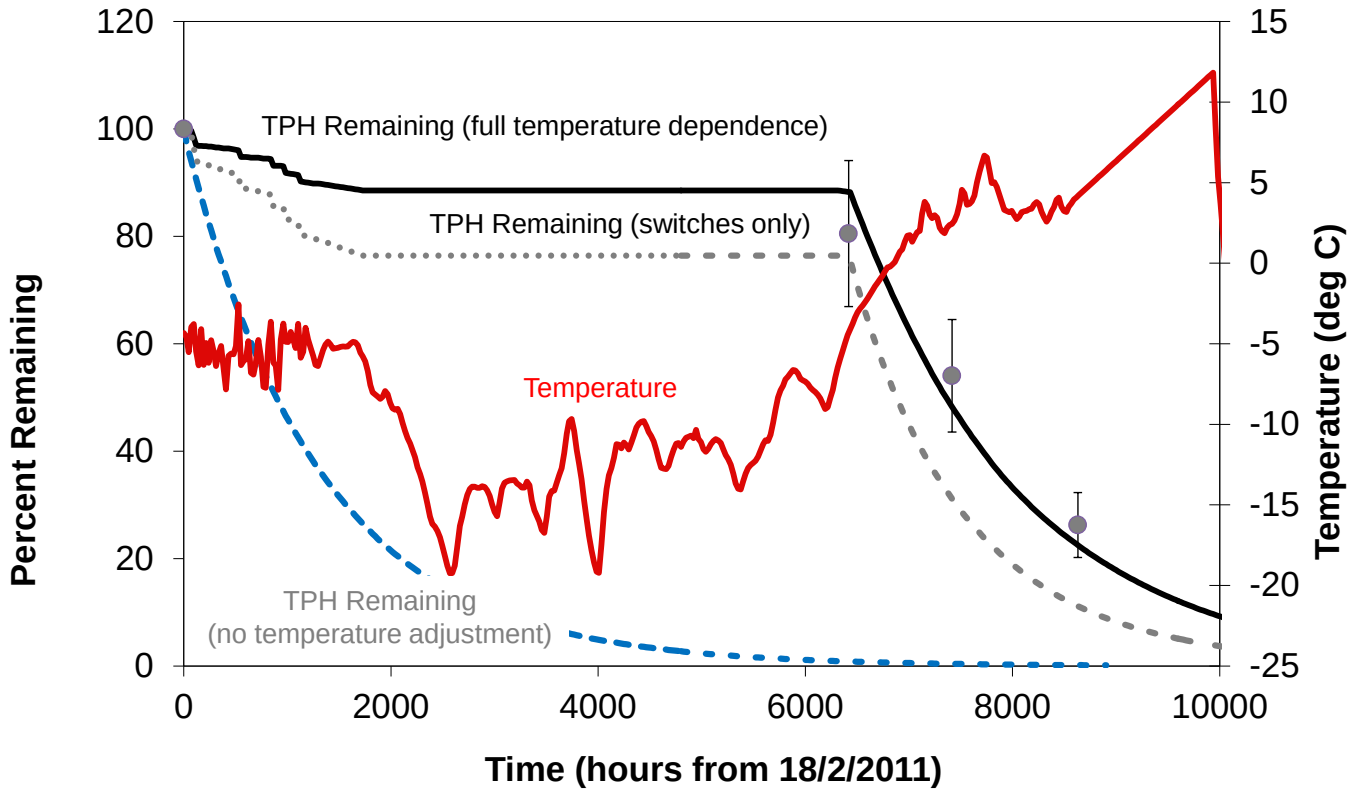

Figure 1 Mean measured (symbols left axis) and predicted (black solid line, left axis) TPH concentration remaining for all five biopiles at Casey Station. Also shown is mean biopile temperature (red line, right axis), the predicted TPH remaining with no temperature adjustment (dashed line) and the predicted TPH remaining with degradation and volatilisation switched off during the winter but with degradation and partitioning otherwise not temperature-adjusted (dotted line). Error bars show the mean ± 1 standard deviation).

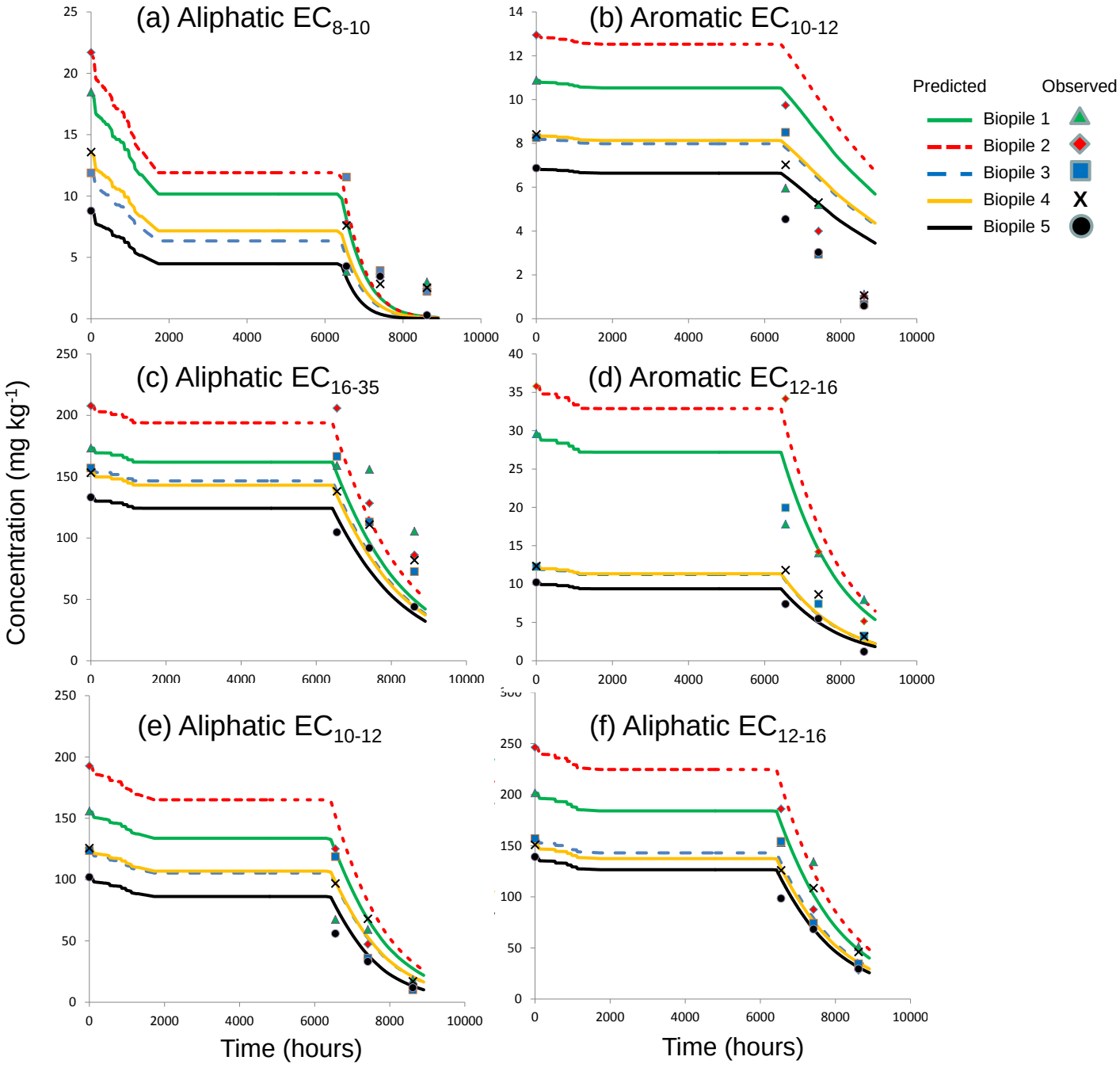

Figure 2 Measured and predicted concentrations of six hydrocarbon fractions remaining in each of the five biopiles at Casey Island.

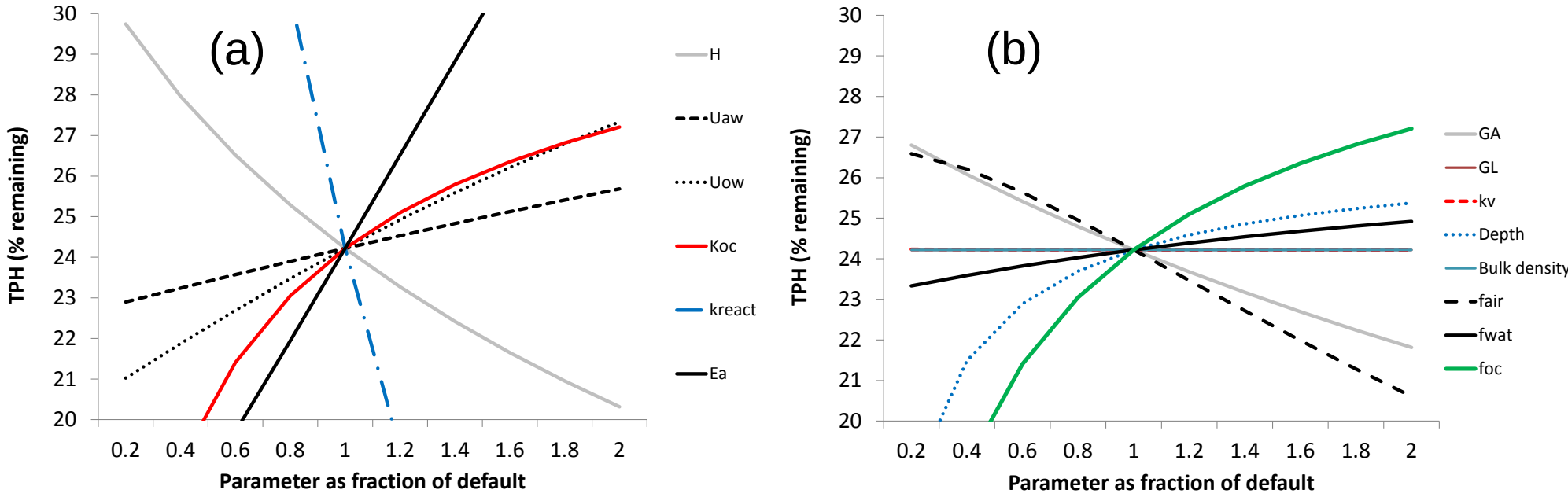

Figure 3 Predicted TPH remaining in Biopile 1 with systematic changes in (a) chemical-specific parameters and (b) system-specific parameters in increments of 20% above and below their default values, with all other parameters kept at their default values. Model sensitivity to a particular parameter is given by the slope of the line. (GA: air flow rate; GL: water flow rate; k_v: partial mass transfer on the air side of the air-soil interface; f_{air}: volume fraction of air; f_{wat}: volume fraction of water; f_{oc}: organic carbon content of the soil).